Journal of
Mechanical
Science and
Technology

Journal of Mechanical Science and Technology 21 (2007) 1172~1177

Development of Speed Reducer with Planocentric Involute Gearing Mechanism

Moon-Woo Park[a,*], Jae-Hoon Jeong[b], Jeong-Hyeon Ryu[a],
Hyoung-Woo Lee[c], Noh-Gill Park[c]

[a]*Department of Mechanical Design Engineering, Graduate School, Pusan National University, Jangjeon-Dong, Geumjeong-Gu, Busan, Korea*
[b]*SsangYong Motor Company, Chilkoi-Dong, Pyeongtaek, Gyeonggi-Do, Korea*
[c]*School of Mechanical Engineering, Pusan National University, Jangjeon-Dong, Geumjeong-Gu, Busan, Korea*

(Manuscript Received December 18, 2006; Revised May 23, 2007; Accepted May 29, 2007)

Abstract

A new speed reducer with the planocentric involute gearing mechanism, which can be replaced with a cycloid drive, is developed. This speed reducer eliminates some significant disadvantages of the cycloid drive, which are difficulty in not only designing and manufacturing the tooth profile but also meshing the gears to maintain an accurate center distance. In this paper, to avoid tooth tip interference between internal and external gears and maximize a speed reduction ratio, a pressure angle, a tooth height, a profile shifting factor and the number of teeth are simulated. We manufacture a prototype based on these simulated results of the design specifications (the rated power of 350watts, rated speed of 3600rpm and speed reduction ratio of 41:1), of which the overall size is Φ146mm×95.2mm. A power efficiency test of the prototype is carried out to compare with the cycloid drive.

Keywords: Gear; Speed reducer; Planetary gear; Planocentric; Involute; Cycloid drive

1. Introduction

Typical speed reducers used widely in industry, which have not only relatively high speed reduction but compactness, have been known as the planetary gear reducer, cycloid drive and harmonic drive. The planetary gear reducer has the advantage of easiness of designing and machining the involute tooth profile as well as little influence of the manufacturing and assembly errors. However, it is difficult to maximize a speed reduction ratio because of the tooth tip interference (Lynwander, 1983). Whereas, the cycloid drive, which uses the planocentric cycloid gearing mechanism, has a higher speed reduction ratio than one of the planetary gear reducer. The designing and machining process of the cycloid gear tooth are very difficult and the manufacturing and assembly errors between the cycloid gears and pins (or rollers) seriously affects in a backlash; mesh to maintain an accurate center distance is important (Lai, 2006). The harmonic drive is used for precision mechanisms required a more higher speed reduction ratio, a little backlash and high compactness, but it has the large moment of inertia due to the wave generator operation and relatively low power effi-ciency. (Calson, 1985)

In this paper, we developed a new speed reducer with the planocentric involute gearing mechanism which can be replaced with the cycloid drive; the speed reducer can not only have the advantages of the planetary gear reducer but eliminate the above sig-

*Corresponding author. Tel.: +82 51 510 1475, Fax.: +82 51 514 7640
E-mail address: munu@pusan.ac.kr

nificant disadvantages of the cycloid drive. The key to design the speed reducer is to avoid the tooth tip interference between the internal and external gears and maximize a speed reduction ratio. Therefore, the objective function is to maximize a speed reduction ratio and the design constraints are considered to set limits to the overall size, contact ratio and bending and contact stresses of the gears. A prototype of the speed reducer with the rated power of 350watts, rated speed of 3600rpm and speed reduction ratio of 41:1 is optimally designed and manufactured for industrial robots. A power efficiency test of the prototype is carried out to compare with the cycloid drive.

2. Mechanism layout

2.1 Kinematic diagram

The mechanism of the new speed reducer is similar to one of the cycloid drive, because the planocentric gearing mechanism is used. The input shaft has two cranks with phase difference of 180°, which are inserted into bearings of the two planetary gears, respectively. The ring gear is fixed to the case. The carrier assembly, which consists of the carrier pins, carrier and its output shaft, is designed to transfer a pure rotation of the planetary gears to the central axis of the output shaft. Bearings are installed at the branches between the front of the input shaft and frontal case, between the frontal crankshaft and frontal planetary gear, between the rear crankshaft and rear planetary gear, and between the rear of the input shaft and case. The case is fixed to a frame or an external structure.

For the speed reducer, a speed reduction ratio can be deduced as (Maiti et al., 1996)

$$i_{12} = -\frac{z_p}{z_r - z_p} \tag{1}$$

Where

z_p : the number of teeth of the planetary gear

z_r : the number of teeth of the ring gear

To maximize a speed reduction ratio, the number of teeth of the planetary gear should be large as many as possible and the difference of the teeth number between the ring and planetary gears should be small as many as possible.

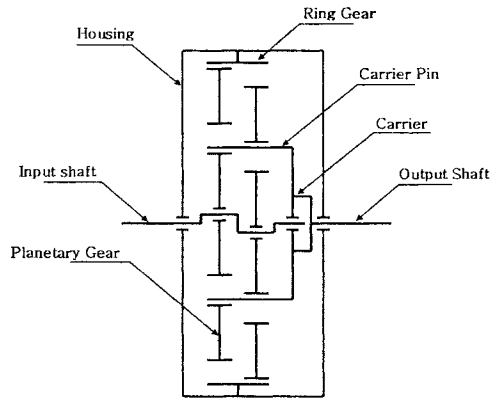

Fig. 1. A kinematic diagram of the planocentric speed reducer.

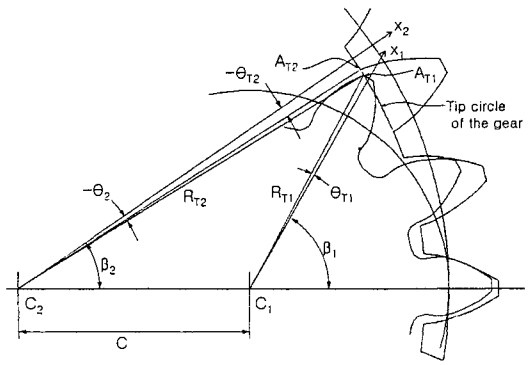

Fig. 2. Checking the tooth tip interference.

2.2 Geometrical considerations in design

The geometric relationship of the tooth tip interference between the ring and planetary gears can be shown in Fig. 2. The tooth tip interference occurs during engagement and disengagement gearing. To prevent a possibility that the tooth tip interference occurs, the path of A_{T1} must clear the point of A_{T2} by adequate margin. The A_{T1} and A_{T2} are the intercepted points between the tip circles of the ring and planetary gears. Thus, a condition that tooth tip interference doesn't occur is determined by arc length between the points of A_{T1} and A_{T2} which is more than 0.05 times as much as the gear module. (Colbourne, 1987)

$$\widehat{A_{T1}A_{T2}} = R_{T2}\left|\theta_{T2} - \theta_2\right| \geq 0.05m \tag{2}$$

Where

R_{T2} : Radius of the tip circle of the gear

θ_{T2} : Polar angle of the point A_{T2}

θ_2 : Polar angle of the point A_{T1} relative to the ring gear

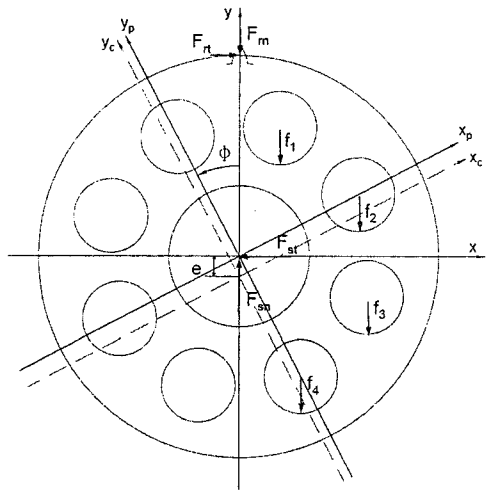

Fig. 3. A free body diagram of the frontal planetary gear.

The variables (R_{T2} , θ_{T2} and θ_2) of the Eq. (2) are functions of the gearing parameters which are the pressure angle, gear module, number of teeth, profile shifting factors, tooth height, etc for the ring and planetary gears. From the Eq. (2), tooth tip interference is verified if these gearing parameters are given.

2.3 Strength analysis

Figure 3 shows a free body diagram of the frontal planetary gear on loading. The transmitted forces (F_{rt}, F_m) are acting on the line of action of the gear pair. In addition, the bearing reaction forces (F_{st}, F_{sn}) are generated from the frontal crankshaft. The reaction forces (f_i, i=1,2,...N/2) are applied from the carrier pins of which total number is N. Neglecting inertia forces, we have three force and moment equilibrium conditions as follows;

$$F_{rn} + F_c = F_{sn} \tag{3}$$

$$F_{rt} = F_{st} \tag{4}$$

$$F_{rt} r_p = F_c r_c \sum_{i=1}^{N/2} \beta_i \sin(i\lambda - \phi) \tag{5}$$

Where

$$F_c = \sum_{i=1}^{N/2} f_i \,, \quad \beta_i = \frac{f_i}{F_c} \,, \quad \lambda = \frac{4\pi}{N} \,, \quad 0 \le \phi < \lambda$$

$$F_{rt} = \frac{1}{2}\frac{T_0}{r_p}$$

T_0: torque acting on the output shaft
r_p: a pitch circle radius of the planetary gear
r_c: a pitch circle radius of the carrier pins

The relationship of the force and deformation between the carrier pins and pin holes is based on the Hertzian contact theory. (Pillkey, 1994)

$$f_i = C\Delta_i^r \tag{6}$$

Where

$$\Delta_i = r_c \Delta\phi \sin(i\lambda - \phi)$$

Using Eqs. (3)~(6), the bearing reaction force is given as follows;

$$F_s = \sqrt{F_{st}^2 + F_{sn}^2} = \sqrt{1 + \left(\eta \frac{r_p}{r_c} + \tan\alpha\right)^2}\, F_{rt} \tag{7}$$

Where;

$$\eta = \frac{\sum_{i=1}^{N/2} \sin^{r+1}(i\lambda - \phi)}{\sum_{i=1}^{N/2} \sin^{r}(i\lambda - \phi)}$$

Bending stresses (S_t) of the tooth root fillet and contact stresses (S_c) on the surface of the gear teeth are calculated by the following AGMA stress equations.

$$S_t = \frac{W_t K_s}{K_v}\frac{1.0}{Fm}\frac{K_s K_m K_B}{J} \tag{8}$$

$$S_c = C_p \left[\frac{W_t C_a}{C_v}\frac{C_s}{d_p F}\frac{C_m C_f}{I}\right]^{1/2} \tag{9}$$

Where

$$W_t = F_{rt}$$

3. Conceptual design

3.1 Optimal design process

To maximize a speed reduction ratio, design para-

meters listed in Table 1 are considered. The specifications to design the new speed reducer are considered as the same specifications as the cycloid drive named by Sumitomo CNH-6095-43 listed in Table 2. The overall size is limited to be Φ160 mm×110 mm as referred to Sumitomo CNH-6095-43. Efficiency is available in case of over 80% and allowable bending and contact stresses of gears, which are ones of the chromium-molybdenum alloy steel (AISI4140), are limited to be 30 kgf/mm^2 and 77 kgf/mm^2, respectively. (Harvey, 1985)

Design of the new speed reducer is carried out by the algorithm of the simple optimal design checking the tooth tip interference, stresses, contact ratio, etc. The detail procedure is listed in Table 3.

Table 1. Design parameters.

Gears	Module	m
	Pressure angle	α
	Teeth numbers of gears	Z_p, Z_r
	Addendum and dedendum	h_a, h_d
	Profile shift factosr	X_p, X_r
	Face width	F
Carrier	Number of carrier pins	Z_c
	Radius of carrier pin	r_e
	Length of carrier pin	l_e
	Pitch circle radius of carrier pin	r_c

Table 2. Design specifications.

Speed ratio	41:1
Rated power (Watt)	350
Rated input speed (rpm)	3600

Table 3. Design algorithm.

1. choose the teeth numbers
2. calculate a speed reduction ratio and skip if it is larger than specified one
3. choose common parameters (module and pressure angle) with prescribed ranges of the rack, tooth height and profile shifting factors for the gears
4. check the tooth tip interference and skip if Eq. (2) is not satisfied.
5. check a contact ratio and skip if it is less than 1.2
6. calculate the transmitted force acting on the planetary gear for the rated power and input speed listed in Table 1.
7. choose the width of the planetary gear
8. check a bending and contact stresses of the gears and skip if these are larger than prescribed allowable ones, respectively.
9. calculate the overall diameter of the ring gear and skip if it is larger than prescribed one
10. Among the selected feasible solution, choose the design parameters to maximize the speed reduction ratio and minimize the overall size.

3.2 Design results

With difference of the teeth number of 4; the 171 teeth number of the ring gear and 167 teeth number of the planetary gear, the new speed reducer having the speed reduction ratio of 41:1 is designed as listed in Table 4. The significant performances of the designed speed reducer are compared with ones of the benchmark cycloid drive (CNH-6095-43) in Table 5. The contact and bending stresses of the designed speed reducer listed in Table 5 are calculated by the AGMA stress equations [Eqs. (8) and (9)]. The contact stress and bearing reaction force of the cycloid drive are calculated by the research of Sung-Chul Lee et al. (1987). The contact stress is nearly twice high but the bearing reaction force has decreased by 19% and the overall size is about the same.

The weak points of stresses are checked by the finite element method (FEM) software (ANSYS). Figure 4 shows the bending stress of the tooth root fillet on condition that the maximum load is acting on the pitch point of the planetary gear. The maximum bending stress of the tooth fillet is 23.25 kgf/mm^2. in addition, Fig. 5 shows a contact stress between the planetary and ring gear and the maximum contact

Table 4. Design results.

Gears		Carrier	
m	0.75 mm	Z_c	4
α	30 °	r_e	10 mm
Z_p	167	l_e	50 mm
Z_r	171	r_c	42 mm
h_a	0.75 mm		
h_d	0.75 mm		
X_p	0		
X_r	0.05		
F	12 mm		

Table 5. Comparisons to the cycloid drive.

	Designed Speed Reducer	Cycloid Drive (CNH-6095-43)
Bending stress of gears (kgf/mm^2)	21.1	-
Contact stress of gears (kgf/mm^2)	28.2	12.9
Bearing reaction force (kgf)	125.0	154.9
Overall size (mm)	Φ146×95.2	Φ145×100

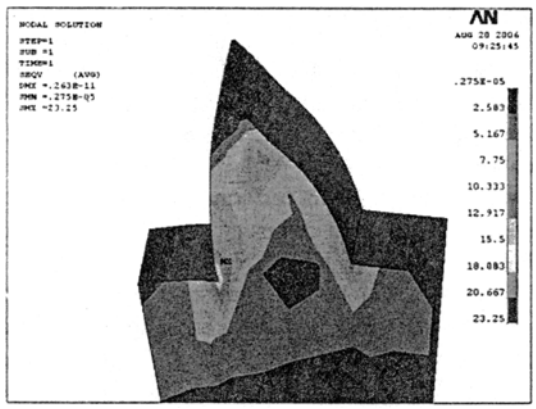

Fig. 4. A bending stress of the planetary gear.

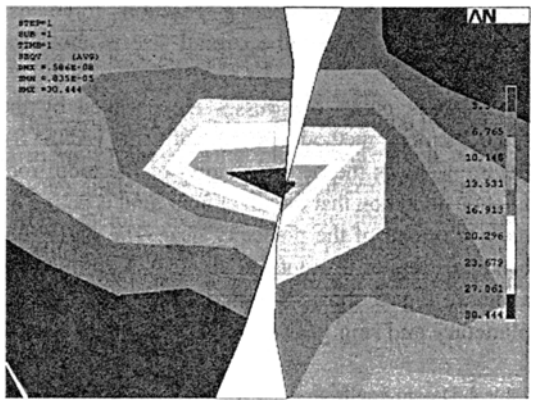

Fig. 5. A contact stress between the planetary and ring gears.

stress is 30.44 kgf/mm^2. These stresses are similar to calculated values by the AGMA stress equations so that the speed reducer is safely designed.

4. Prototype evaluation

4.1 Detail design for prototype

Based on the results of the conceptual design listed in Table 4, we have done a detail design. The input shaft having a crankshaft with eccentricity of 1.5mm and output shaft connected to the carrier are designed. We used the software of COBRA (Advanced rotating machinery Dynamics, 1994) to verify the fatigue life of the five bearings according to the calculated bearing radial forces. Based on the reaction forces, the four carrier pins inserted into roller bushes (dry bearings) which are in contact with pin holes of the planetary gears are designed. A solid model is constructed as shown in Fig. 6 by commercial CAD software. (Pro/Engineer)

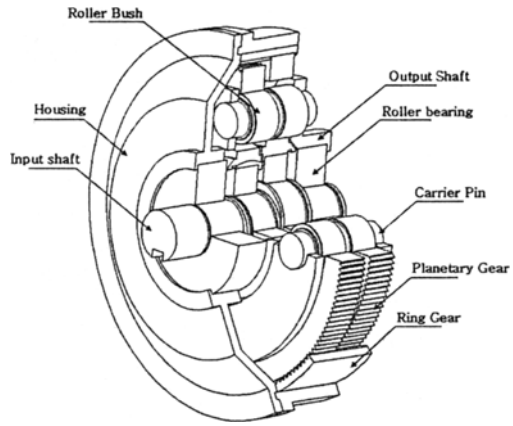

Fig. 6. A solid model of the planocentric speed reducer.

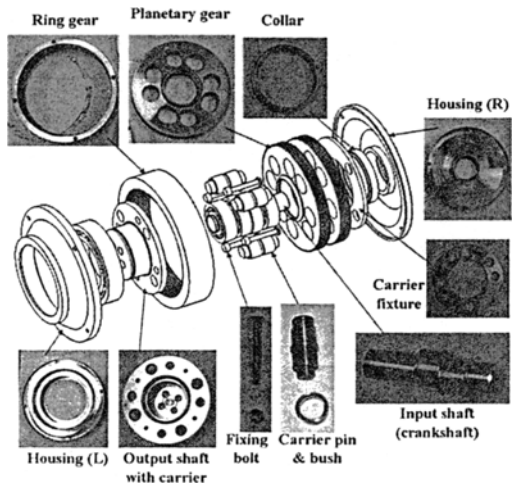

Fig. 7. Manufactured components of the planocentric speed reducer.

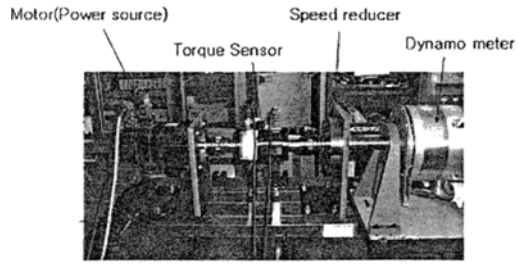

Fig. 8. The test-bench for the planocentric speed reducer.

4.2 Prototype manufacturing

Figure 7 shows manufactured components of the speed reducer. The major components; the planetary and ring gears are machined by a typical hobbing machine. The input shaft (the crankshaft), output shaft (the carrier) and carrier pins are machined by CNC machine tools and the other components are ma-

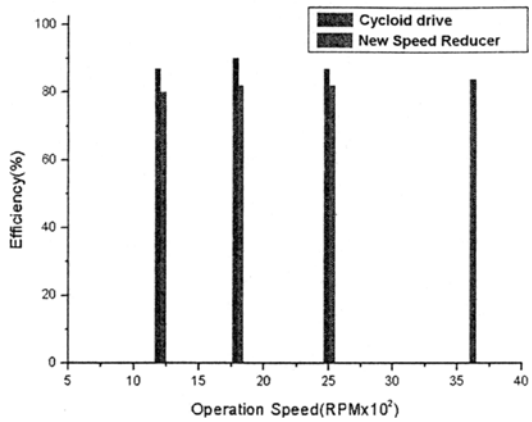

Fig. 9. A comparison of measured efficiency between the planocentric speed reducer and cycloid drive.

chined by a generic lathe and milling machine.

4.3 Performance test

Figure 8 shows a test-bench to measure power transmission efficiency of the prototype. The test-bench consists of a power source (AC servo motor), torque-sensor and dynamometer. The input shaft of the prototype is directly connected to the torque-sensor and the output shaft is also directly connected to the dynamometer. A test to measure power efficiency of the prototype is carried out under condition of constant output torque (dynamometer brake torque) of 38N-m and variable input speeds. Figure 9 shows efficiency of the prototype and benchmark cycloid drive (CNH-6095-43) measured on the same condition. The power efficiency of the prototype is measured as high as 80%. According to a comparison of the efficiency between the prototype and cycloid drive, a difference of the efficiency is about 5%, which is slight. Therefore, we consider that the new speed reducer is suitable to be replaced with the cycloid drive and used widely in industry.

5. Conclusion

We developed the new speed reducer with the planocentric involute gearing mechanism, which can be replaced with the cycloid drive. To avoid the tooth tip interference and maximize a speed reduction ratio, a pressure angle, a tooth height, a profile shifting factor and the number of teeth are simulated. We manufactured the prototype with these simulated results for the design specifications and carried out its efficiency test to compare with the cycloid drive. (RV-20)

(1) Within the overall size of Φ146 mm×95.2 mm, the speed reducer with rated power 350 watt, rated speed 3600 rpm, and a speed reduction rate of 41:1 can be designed.

(2) The module and teeth numbers of the ring and planetary gears are 0.75, 171 and 167, respectively. The pressure angle is determined to be 30° to avoid the tooth tip interference.

(3) The power efficiency of the prototype is measured as high as 80%. A difference of the efficiency between the prototype and cycloid drive is about 5%, which is slight. The prototype is suitable to be replaced with the cycloid drive.

(4) The key point of the new model is regarded as to be economic to manufacture due to little influence of a manufacturing and assembly errors.

References

Advanced Rotating Machinery Dynamics (Rotor bearing, Technology & Software), 1994, "COBRA," USA.

AGMA, 1988, "Fundamental Rating Factors and Calculation Methods for Involute Spur and Helical Gear Teeth," ANSI/AGMA 2001-B886.

AGMA, 1989, "Geometry Factors for Determining the Pitting Resistance and bending Strength of Spur, Helical and Herringbone Gear Teeth," AGMA 908-B89.

Calson, J. H., 1985, "Harmonic Drive for Servo Mechanisms," *Machine Design*, Vol. 6 pp. 102~106.

Colbourne, J. R., 1987, "The Geometry of Involute Gears," *Springer-Verlag New York.*

Peter Lynwander, 1983, "Gear Drive Systems," *Marcel Dekker, Inc.*, pp.293~323.

Philip, D. Harvey and Editors, 1985, "Engineering Properties of Steel," *American Society for Metals, Metals Park*, Ohio 44073, second printing.

MAITI, R. and ROY, A.K., 1996, "Minimum Tooth Difference in Internal-external Involute Gear Fair," *Mech. Mach. Theory* Vol. 31. No. 4, pp. 475~485.

Lee, Sung-Chul, Oh, Park-Kyoun and Kwon, Oh-Kwan, 1987, "A Study on the Design of the Torque Driver Used in Industrial Robot," *Journal of the KSLE*, Vol. 3, No. 2, pp. 72~80.

Ta-Shi Lai, 2006, "Design and Machining of the Epicycloid Planet Gear of Cycloid Drives," *Int. J. Adv Manuf Technol*, Vol. 28, pp. 665~670.

Walter D. Pillkey, 1994, "Formulas for Stress, Strain and Structual Matrices," *J. Wiley New York.*